Analysis of retrieval accuracy and spatial-temporal variation of chlorophyll-a concentration in Bohai Sea based on GOCI

Jing-wen Hu, Xiao-yan Liu, Qi-xiang Wang, Xin Li, Wen-long Dong, Wei-qi Lin, Jun-yue Zhang, Ming-yu Li and Zhi-hong Wu

***Abstract*—Bohai Sea is China's inland sea, its complex marine and atmospheric optical properties pose a challenge to the application of satellite data to retrieve chlorophyll-a concentration (CHLA) with high accuracy. The high accuracy retrieval results of CHLA require simultaneous consideration of the adaptability of atmospheric correction algorithms and CHLA retrieval models. In this study, four atmospheric correction methods (the standard atmospheric correction algorithms of GDPS1.4.1 and GDPS2.0, the standard near-infrared atmospheric correction algorithm of NASA (Seadas_Default), and Management Unit of the North Sea Mathematical Models (Seadas_MUMM)) and four CHLA retrieval models (OC2, YOC, OC3G, OC2M-HI) were selected in the process of applying GOCI (Geostationary Ocean Color Imager) data to retrieve CHLA in Bohai Sea. Based on the in-situ data, the adaptability of their pairwise combinations in retrieval of CHLA in Bohai Sea was evaluated. The results indicate that the OC2 and OC3G models significantly overestimated the CHLA. The combination of the Seadas_Default atmospheric correction algorithm with the YOC CHLA retrieval model, or the combination of the Seadas_MUMM atmospheric correction algorithm with the YOC CHLA retrieval model, is more suitable for the retrieval of CHLA using GOCI data in Bohai Sea. Additionally, this study shows that the CHLA obtained based on the data from 8-scene GOCI data were different to the data obtained based on single-scene GOCI data (approximating traditional polar-orbiting satellite sensor data) in daily, monthly, and yearly average results. The monthly mean difference between the two is the most significant, ranging from -0.66 to 1.49 ug/l.**

***Index Terms*—atmospheric correction, GOCI, Bohai Sea, chlorophyll-a**

This work was supported in part by the Open Foundation of Weifang Key Laboratory of Satellite Remote Sensing Intelligent Interpretation Technology (Grant No. SYS202303), in part by the National Key Research and Development Program of China (Grant No. 2019YFC1408003), and the Natural Science Foundation of Shandong Province (Grant No. ZR2023QD023, ZR2022QD061, ZR2021QD135). (*Corresponding author: Zhi-hong Wu.)*

Jingwen Hu is with the Weifang Key Laboratory of Satellite Remote Sensing Intelligent Interpretation Technology, Weifang 261021, China, and with the Shandong Marine Forecast and Hazard Mitigation Service, Qingdao 266000, China (email: hujingwen@shandong.cn)

Xiaoyan Liu, Weiqi Lin, Junyue Zhang and Mingyu Li are with the Institute of Oceanographic Instrumentation, Qilu University of Technology (Shandong Academy of Sciences), Qingdao 266000, China (e-mail: liuxiaoyan@qlu.edu.cn; linwq0908@163.com; junyuezhang2024@163.com; limingy0112@163.com).

Qi-xiang Wang, Wen-long Dong, and Zhi-hong Wu are with the Shandong Marine Forecast and Hazard Mitigation Service, Qingdao 266000, China (e-mail:wqxbx@163.com;dongwenlong529@163.com;wuzhihong@aliyun.com).

Xin Li is with the Weifang Marine Development Research Institute, Weifang 261021, China (e-mail: maliao0919@163.com).

I. INTRODUCTION

BOHAI Sea (Fig. 1) is a semi-enclosed inland sea surrounded by land on three sides, and it is the only one of its kind in China. It has numerous rivers along its coast, and it serves as a convergence point for three of China's seven major water systems: the Yellow River, Hai River, and Liao River systems. With the development and construction of the 13 coastal cities around the Bohai Sea, the amount of land-based pollutant emissions has been increasing year by year, greatly impacting the marine ecological environment quality of the Bohai Sea [1-4]. In recent years, in order to promote the sustainable development of the Bohai Sea and the rational utilization of marine resources, relevant government authorities in China have introduced a series of policies and measures. Therefore, it is of great significance to conduct research on the spatial and temporal variations of key ecological factors and water quality parameters in the Bohai Sea to sustainably monitor and evaluate the ecological environment regulatory work, including monitoring the concentration of chlorophyll-a in the Bohai Sea.

Chlorophyll-a concentration of the water is a key indicator of marine phytoplankton biomass, and one of the basic parameters for measuring marine net primary production and eutrophication. Studying its spatial-temporal changes provides necessary reference for in-depth analysis of global hot issues such as changes in marine ecosystems, global carbon cycles, and climate change [5, 6]. Traditional observations of chlorophyll-a concentrations are often conducted through marine buoys or aerial surveys, which are not only time-consuming and laborious but also difficult to conduct large-scale investigations [7, 8]. Remote sensing technology, with its fast imaging speed, multiple spectral bands, wide imaging range, long time series, and low economic cost, has rapidly become an important means of obtaining ecological information such as chlorophyll-a concentrations [9]. In recent years, mainstream remote sensing inversion algorithms for chlorophyll-a concentrations are mostly based on empirical algorithms and semi-analytical algorithms [10-23], and some researchers have tried to estimate chlorophyll-a concentrations using machine learning methods such as neural networks [24, 25]. But overall, the primary reliance for the retrieval of

chlorophyll-a concentration using satellite data is the remote sensing reflectance (R_{rs}) data of the water, for example, the OC2 algorithm [26] and OC2M-HI algorithm [27] are both based on the R_{rs} data at 490nm and 555nm wavelengths, YOC algorithm [28] is based on the R_{rs} data at 412nm, 443nm, 490nm, and 555nm wavelengths, and OC3G algorithm [29] is based on the R_{rs} data at 443nm, 490nm, and 555nm wavelengths. High-quality marine remote sensing research requires precise R_{rs} data as a basis [30, 31]. Obtaining R_{rs} data of the water from satellite sensor data requires atmospheric correction. Effective atmospheric correction algorithms proposed by international scholars for near-shore case II turbid water include dark pixel method [32, 33], bright pixel method [34, 35], neural network method [36-38], spectral matching optimization method [39-41], etc. Research shows that there are significant differences between R_{rs} data obtained from the same satellite data when using different atmospheric correction algorithms in the same sea area [42], and differences in ecological parameter retrieval algorithms for the same sea area can also cause huge differences in retrieval results [16]. But there is still a lack of literature on wide-ranging joint evaluation of the accuracy of specific sea area ecological parameter retrieval by unifying atmospheric correction algorithms and ecological parameter retrieval algorithms. Currently, the number of available atmospheric correction algorithms and chlorophyll-a concentration retrieval algorithms is numerous, and different combination pairs may cause differences in retrieval accuracy. Therefore, evaluating the reliability of various chlorophyll-a concentration retrieval algorithms under different atmospheric correction algorithms has important application value. In addition, most of the spatiotemporal change analyses of chlorophyll-a concentration by domestic and foreign scholars are based on polar-orbiting satellite data (such as MODIS, SeaWiFS, etc.) [43, 44]. However, the studies about Marine ecological elements (such as transparency, sea surface salinity, and chlorophyll-a, etc.) based on GOCI show that the hourly variation difference can not be ignored [45-48]. Therefore, it is significant to compare the spatiotemporal changes of chlorophyll-a concentration in Bohai Sea based on the multi-frequency observations of GOCI with the results based on single observation data.

GOCI, the primary sensor mounted on the geostationary satellite COMS, provides up to 8 daily observations (GOCI II provides 10 daily observations). In comparison to polar-orbiting satellites, GOCI significantly enhances the temporal resolution and spatial coverage of remote sensing data. This improvement enables the monitoring of short-term changes in coastal water quality and large algae. It is also particularly crucial for studying the long-term variations in bio-optical parameters [49, 50].GDPS (GOCI Data Processing System) is a specialized software designed for the analysis and processing of GOCI sensor data, specifically allowing for atmospheric correction. KOSC (Korea Ocean Satellite Center) has, to date, offered six versions of GDPS (GDPS 1.1, GDPS 1.2, GDPS 1.3, GDPS 1.4, GDPS 1.4.1, GDPS 2.0) to users worldwide free of charge. SeaDAS is a dedicated software for processing water color remote sensing data. It performs atmospheric correction on satellite data and uses NASA's standard atmospheric correction algorithm as its default (SeaDAS_Default). Additionally, SeaDAS provides the MUMM atmospheric correction algorithm (SeaDAS_MUMM) for user.

In this study, in the process of retrieval of chlorophyll-a concentration in Bohai Sea using GOCI data, four operational atmospheric correction algorithms and four chlorophyll-a concentration retrieval algorithms were used for pairwise combination. Then 16 groups of retrieved results were compared with the in-situ chlorophyll-a concentration data respectively to select the most suitable combination of atmospheric correction and chlorophyll-a concentration retrieval algorithm for the Bohai Sea. The selected algorithm combination was applied to retrieve chlorophyll-a concentration using GOCI data from April 2011 to March 2021, and the temporal and spatial changes of chlorophyll-a concentration in Bohai Sea in the ten years were analyzed.

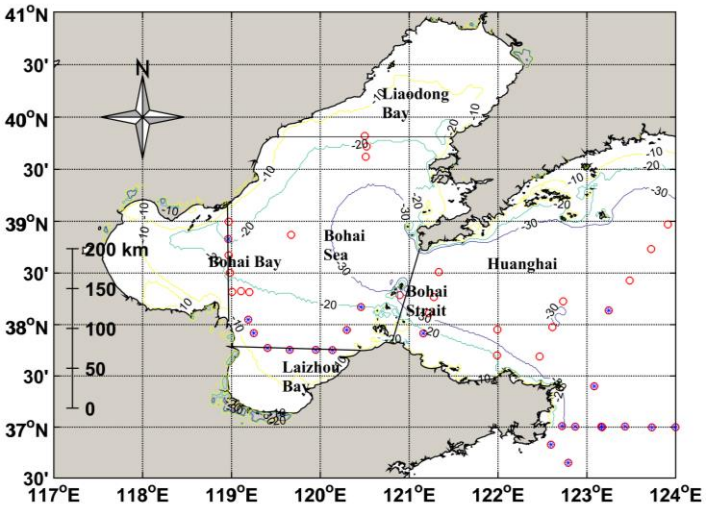

Fig. 1. The location map of Bohai Sea. The red dots represent the locations of the measurement stations, and the contour lines represent the water depth. The bule dots represent the stations can be paired with the data retrieved from GOCI under clear skies.

II. DATA

A. In-situ Data

The field sampling and laboratory measurement of chlorophyll-a concentration were conducted in the Bohai Sea on April 30, 2014, May 3, 2014, May 12, 2014, September 10, 2015, May 16, 2017, and March 9-12, 2018. A total of 42 measured station data were obtained. The red dots in Fig. 1 represent the locations of the measurement stations. And 21 measured chlorophyll-a concentration of these stations (blue dots in Fig. 1) can be paired with the data retrieved from GOCI under clear skies. The measurement method for chlorophyll-a concentration was used spectrophotometry. The specific procedure involved obtaining 2-5L of seawater sample, adding 3ml of magnesium carbonate suspension, mixing thoroughly, and filtering through a 0.45 um cellulose acetate membrane filter. The filtered membrane was placed in a centrifuge tube, and 10ml of acetone solution was added. The mixture was shaken and left to stand in a refrigerator for 14-24 hours to extract the chlorophyll-a concentration. The

supernatant of the extraction (v ml) was transferred to a measurement cell, and acetone solution was used as a reference. The absorbance values were measured at wavelengths of 750nm, 664nm, 647nm, and 630nm using a spectrophotometer. The measurement at 750nm was used to correct for the turbidity of the extraction solution. If the absorbance value at a 1cm measurement cell exceeded 0.005, the extraction solution needed to be re-centrifuged. The absorbance values at 664nm, 647nm, and 630nm were subtracted from the absorbance value at 750nm to obtain the corrected absorbance values (E664, E647, E630). The concentration of chlorophyll-a was then calculated using equation (1).

$$CHLA=(11.85\times E664-1.54\times E647-0.08\times E630)\times v/(V\times L) \quad (1)$$

The unit of CHLA is μg/l, where v represents the volume of the sample extraction (ml), V denotes the actual volume of seawater sample used (l), and L stands for the path length of the measurement cell (cm).

B. GOCI Data

The swath width of GOCI imagery is 2,500 × 2,500 km, covering the Bohai Sea, Yellow Sea, and parts of the East China Sea. It has a spatial resolution of 500m and a spectral range of 0.412-0.865um, including six visible light bands and two near-infrared bands. It acquires 8-scene observation data per day, from Beijing local time 8 a.m. to 15 p.m., with one scene per hour. The L1B data used in this study were provided by the KOSC for the period from April 1, 2011, to March 31, 2021.

C. GMI Data

The GMI microwave radiometer was carried on the Global Precipitation Measurement (GMP) satellite and was successfully launched on February 27, 2014. In this study, we selected the global monthly average data of GMI from January 2015 to January 2020, which can provide data values such as sea surface temperature, rain rate and wind speed. The download address is: https://www.remss.com/missions/gmi/.

III. ALGORITHM

A. Atmospheric correction algorithm

The target of atmospheric correction is to get surface water reflectance, $\rho_w(\lambda)$, extracted from the top of atmosphere ($\rho(\lambda)$) measured by satellite. Ignoring the surface-reflectance from sun-glint and whitecaps, $\rho(\lambda)$ can be described as follows[51]:

$$\rho(\lambda) = \rho_r(\lambda) + \rho_a(\lambda) + t\rho_w(\lambda) \quad (2)$$

where ρ_r is the Rayleigh multiple-scattering reflectance in the absence of aerosols, and ρ_a is the aerosol multiple-scattering reflectance in the presence of air molecules. And t is the diffuse transmittance of the atmosphere from the sun to the sea surface and from the sea surface to the sensor.

$\rho_r(\lambda_0)$ can be obtained based on pre-calculations through radiative transfer simulations. Then the $\rho_a(\lambda_0)$ of the corresponding NIR bands and β in equation (3) can be calculated by using the measured data $\rho(\lambda_0)$ through equation (2) and equation (3) by assuming the value or ratio relationship of the $\rho_w(\lambda_0)$ of the two NIR bands. Then the $\rho_a(\lambda)$ at any wavelength can be calculated by equation (3), and finally, the $\rho_w(\lambda)$ at any wavelength can be calculated by equation(2).

$$\rho_a(\lambda_i)= (\lambda_i/\lambda_j)^{-\beta}\rho_a(\lambda_j) \quad (3)$$

GDPS is the official software provided by KOSC for processing GOCI data. GDPS1.1 and GDPS1.2 used the empirical relation between the red band and NIR water-leaving reflectance to calculate the NIR reflectance ρ_w (equations (4)) due to the lack of NIR band information in GOCI [52].

$$\begin{aligned}\rho_w(745) &= \sum_{n=1}^{4} j_n \rho_w^n(660)\\ \rho_w(865) &= 1.936\times\rho_w(745)\end{aligned} \quad (4)$$

GDPS1.3 modified the above equations [53]:

$$\begin{aligned}\rho_w(745) &= \sum_{n=1}^{6} j_n \rho_w^n(660)\\ \rho_w(865) &= \sum_{n=1}^{2} k_n \rho_w(745)\end{aligned} \quad (5)$$

The GDPS1.4* mainly updates the software modularization based on the GDPS1.3, without changing the atmospheric correction algorithm [53]. The atmospheric correction of GDPS2.0 takes advantage of the spectral relationship between the reflectance of multiple scattering of aerosols at different wavelengths, called SRAMS (the spectral relationships in the aerosol multiple-scattering reflectance between different wavelengths) to calculate the reflectance contribution of near-infrared multiple scattering directly. Then SRAMS spectra were used to estimate the reflection contribution of the aerosol model in the near infrared band to the visible band [54]. The spectral relationship between the reflection spectra of multiple scattering aerosols and different wavelengths is established by polynomial function (equation 6), and the relations of the spectral segment are summarized in Table 1.

$$\rho_w(\lambda_2) = \sum_{n=1}^{D} c_n \rho_w{}^n(\lambda_1) \quad (6)$$

D represents the calculation order.

TABLE 1. THE RELATIONS OF EACH SPECTRAL BAND

λ1 (nm)	555	555	555	745	745	745	865
λ2 (nm)	412	430	490	555	660	680	745
D	4	4	4	4	3	3	2

Based on this, we used the atmospheric correction algorithm of GDPS1.4.1 and GDPS2.0 to process the GOCI L1B data and got the corrected R_{rs} data.

Additionally, two atmospheric correction algorithms of SeaDAS 8.2 (Seadas_Default and Seadas_MUMM) were selected to process the atmospheric correction on GOCI data, and the corrected R_{rs} data were obtained. The NASA standard atmospheric correction algorithm (i.e., Seadas_Default in this

study) was originally developed by Gordon and Wang [55] in 1994, and was extended its application to case II waters by Stumpf et al in 2003 [56], and further was revised by Bailey and Ahmad et al [57, 58]. NASA uses this algorithm as the default atmospheric correction algorithm of SeaDAS to process the ocean color remote sensing data and provides L2 products for users. The MUMM atmospheric correction algorithm was proposed by Ruddick in 2000,which assumed that the aerosol multiple scattering reflectance ratio of the two near-infrared bands of each pixel is a fixed value and the ratio between reflectance and atmospheric transmission at the two near-infrared bands is constant [59].

B. CHLA retrieval algorithm

Many retrieval models of chlorophyll-a concentration have been proposed and applied in the world currently. This paper selects four representative chlorophyll-a concentration retrieval models, OC2, YOC, OC3G, and OC2M-HI, and matches them with the four atmospheric correction algorithms selected above to analyze their reliability in the sea area studied in this paper.

OC2 is a cubic polynomial algorithm proposed by HOOKER et al. [26] based on the ratio of R_{rs} in the 490nm and 555nm bands. Its algorithm expression is:

$$\mathrm{CHLA} = e_0 + 10^{e_1+e_2\times R+e_3\times R^2+e_4\times R^3} \tag{7}$$

$$R = \log_{10}\left(\frac{\mathrm{R_{rs}}(490)}{\mathrm{R_{rs}}(555)}\right) \tag{8}$$

where, e_0=-0.0929, e_1=0.2974, e_2=-2.2429, e_3=0.8358, e_4=-0.0077.

YOC was obtained by SISWANTO et al. [28] after optimizing the parameters of the chlorophyll-a concentration retrieval algorithm proposed by TASSAN et al. [60]based on measured data. It is a quadratic polynomial algorithm based on the R_{rs} ratio in the 412 nm, 443 nm, 490 nm, and 555 nm bands. Its algorithm expression is:

$$\mathrm{CHLA} = 10^{c_1-c_2\times log_{10}^{(R)}-c_3\times log_{10}^2(R)} \tag{9}$$

$$R = \frac{R_{rs}(443)}{R_{rs}(555)}\left(\frac{R_{rs}(412)}{R_{rs}(490)}\right)^{C_4} \tag{10}$$

where, c_1=0.342, c_2=2.511, c_3=0.277, c_4=-1.012.

OC3G is a fourth-order polynomial algorithm [29] based on the OC4 algorithm [61], which uses the maximum ratio of R_{rs} (443)/R_{rs} (555) to R_{rs} (490)/R_{rs} (555) to establish a fourth-order polynomial algorithm . Its algorithm expression is:

$$\mathrm{CHLA} = 10^{f_0+f_1\times R+f_2\times R^2+f_3\times R^3+f_4\times R^4} \tag{11}$$

$$R = log_{10}\frac{\max[Rrs(443),Rrs(490)]}{Rrs(555)} \tag{12}$$

where, f_0=0.366, f_1=-3.067, f_2=1.93, f_3=0.649, f_4=-1.532.

The OC2M-HI algorithm [27] developed by the members of NASA is also a widely used chlorophyll-a concentration retrieval algorithm, which is a fourth-order polynomial algorithm based on the ratio of R_{rs} in the 490nm and 555nm bands. Its algorithm expression is:

$$\mathrm{CHLA} = 10^{a_1-a_2\times R+a_3\times R^2-a_4\times R^3-a_5\times R^4} \tag{13}$$

$$\mathrm{R} = log_{10}\left(\frac{R_{rs}(469)}{R_{rs}(555)}\right) \tag{14}$$

where, a_1=0.1464, a_2=1.7953, a_3=0.9718, a_4=0.8319, a_5=0.8073. Due to GOCI was not set the band of 469nm, this paper uses interpolation method to obtain R_{rs} data in the 469nm band.

C. Accuracy evaluation

The correlation coefficient r, root mean square error RMSE, and the averaged unbiased percentage difference ε, were calculated to assess the accuracy of validation, and goodness-of-fit as follows:

$$\mathrm{r} = \frac{\sum_{i=1}^{n}\left(X^i_{\text{chla-est}}-\overline{X}\right)\left(Y^i_{\text{chla-mea}}-\overline{Y}\right)}{\sqrt{\sum_{i=1}^{n}\left(X^i_{\text{chla-est}}-\overline{X}\right)^2\left(Y^i_{\text{chla-mea}}-\overline{Y}\right)^2}} \tag{15}$$

$$\mathrm{RMSE} = \sqrt{\frac{1}{\mathrm{n}}\cdot\sum_{i=1}^{n}\left(X^i_{\text{chla-est}}-Y^i_{\text{chla-mea}}\right)^2} \tag{16}$$

$$\varepsilon = \frac{1}{\mathrm{n}}\cdot\sum_{i=1}^{n}\left[X^i_{\text{chla-est}}-Y^i_{\text{chla-mea}}\right]/\left[X^i_{\text{chla-est}}+Y^i_{\text{chla-mea}}\right]*200\% \tag{17}$$

where, the subscript *i* represents an individual data point, and *n* is the number of samples. When used to evaluate the accuracy of the CHLA model, $X_{chla\text{-}est}$ and $Y_{chla\text{-}mea}$ are the estimated and measured values of CHLA respectively.

IV. Results and Analysis

A. Error analysis of retrieved CHLA

Firstly, GOCI L1B data with the same date follow the field sampling data were selected and processed by GDPS1.4.1, GDPS2.0, Seadas_Default and Seadas_MUMM atmospheric correction algorithms respectively, and four groups of R_{rs} data were obtained. Then, OC2, YOC, OC3G, and OC2M-HI retrieval algorithms were used to retrieve the chlorophyll-a concentration of each group of R_{rs} data, and 16 sets of calculation results were obtained by combining four atmospheric correction algorithms with four chlorophyll-a concentration retrieval algorithms. According to the principle of spatial-temporal matching (the spatial range no more than 300m and the time range no more than ±5h), the retrieved chlorophyll-a concentration data were paired with the in-situ chlorophyll-a concentration data for comparative analysis. The specific results were shown in Fig. 2, and different colors of the dots represent different atmospheric correction algorithms we used: black dots represent GDPS1.4.1, red dots represent GDPS2.0, green dots represent Seadas_Default, and blue dots represent Seadas_MUMM.

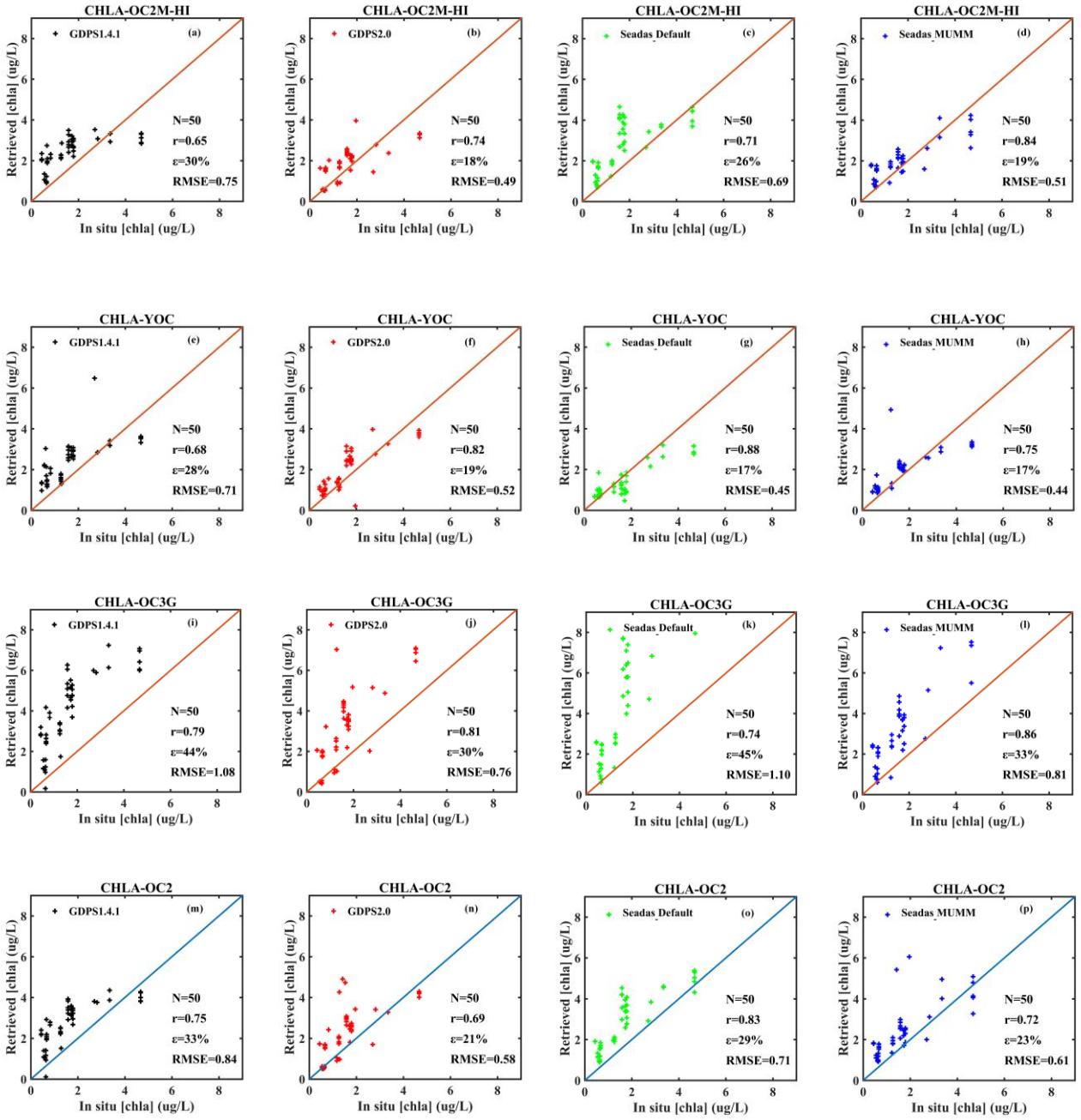

Fig. 2. Comparison figures of 16 sets of retrieved chlorophyll-a concentration data from GOCI with in-situ Data. Fig.(a-d) comparison result between retrieved CHLA data by using OC2 algorithm under four atmospheric correction algorithms and in-situ CHLA data; Fig.(e-h) comparison result between retrieved CHLA data by using YOC algorithm under four atmospheric correction algorithms and in-situ CHLA data; Fig.(i-l) comparison result between retrieved CHLA data by using OC3G algorithm under four atmospheric correction algorithms and in-situ CHLA data; Fig.(m-p) comparison result between retrieved CHLA data by using OC2M-HI algorithm under four atmospheric correction algorithms and in-situ CHLA data.

It can be concluded that when the chlorophyll-a concentration retrieval algorithm is OC2, the accuracy of chlorophyll-a concentration retrieved from GOCI by using GDPS2.0 atmospheric correction algorithm performs slightly better than the other three atmospheric correction algorithms. The correlation coefficient between retrieved chlorophyll-a concentration data from this combined and the in-situ chlorophyll-a concentration data is 0.69, with an average relative error of 21% and a root mean square error of 0.58 (Fig.2(a-d)). When the chlorophyll-a concentration retrieval algorithm is YOC, the performance of the Seadas_Default atmospheric correction algorithm and the Seadas_MUMM atmospheric correction algorithm is comparable, both of which are superior to the other two atmospheric correction algorithms (Fig.2(e-h)). When the chlorophyll-a concentration retrieval algorithm is OC3G, the comparison results between

the chlorophyll-a concentration data obtained from the four atmospheric correction algorithms and the measured data are generally similar, all significantly higher than the measured chlorophyll-a concentration data. This OC3G algorithm has poor adaptability in the Bohai Sea, and the model coefficients need to be optimized and adjusted (Fig.2(i-l)). For the OC2M-HI algorithm, the comparison results between the chlorophyll-a concentration data obtained from the GDPS2.0 atmospheric correction algorithm or the Seadas_MUMM atmospheric correction algorithm and the in-situ chlorophyll-a concentration data are generally similar, and both are superior to the other two atmospheric correction algorithms (Fig.2(m-p)).

It can be seen that for the same chlorophyll-a concentration retrieval model, there are significant differences in the chlorophyll-a concentration values caused by different atmospheric correction algorithms. And the differences between the retrieval results obtained by different chlorophyll-a concentration retrieval models under the same atmospheric correction algorithm also cannot be ignored. In the Bohai Sea area, when applying GOCI data to monitor chlorophyll-a concentrations, it is necessary to simultaneously consider the combined results of atmospheric correction algorithms and chlorophyll-a concentration models. The results of this study show that the performance relationship of each combination are as follows: Seadas_Default_YOC ≈ Seadas_MUMM_YOC > GDPS2.0_OC2M-HI ≈ GDPS2.0_YOC ≈ Sedas_MUMM_OC2M-HI > Other combinations. Considering the doubts raised by some research results regarding the adaptability of NASA's standard atmospheric correction algorithm to case II coastal water bodies [62, 63], this paper used the Seadas_MUMM atmospheric correction algorithm to process GOCI data in the subsequent analysis of chlorophyll-a concentration, and the retrieval model for chlorophyll-a concentration used YOC.

B. GOCI monitoring results of CHLA

GOCI is the first geostationary ocean color satellite sensor of the world. Compared with the conventional polar-orbiting satellite sensors such as Terra/MODIS, Aqua/MODIS, etc., GOCI can acquire 8 scene observations per day (Fig. 3), significantly improving the coverage of daily observations. This study quantitatively and analytically investigates the spatial distribution and temporal variation patterns of chlorophyll-a concentration in the Bohai Sea using high-frequency GOCI data compared to traditional low-sampling-frequency polar-orbiting satellite sensors at daily, monthly, and yearly scales. It is worth noting that considering 04:16 (UTC) time is close to the transit time of most traditional polar-orbiting water-color satellite sensors, the imaging data of GOCI 04:16 (UTC) time is selected in this study to approximate the results of traditional polar-orbiting ocean color satellite sensors (denoted as CHLA_Time_04), and compares it with the average value of the 8 GOCI observations (denoted as CHLA_Time_all) to analyze the differences between the two.

Fig. 3 shows the spatial distribution of chlorophyll-a concentration monitored by eight scenes of hourly imaging data in Bohai Sea on September 13, 2015. It is obvious that the concentration of chlorophyll-a in Bohai Sea is significantly higher from 02:16 to 04:16 than at other times. Especially in the central Bohai Sea, the hourly variation characteristics of chlorophyll-a concentration were significant. Fig. 4(a) shows the standard deviation distribution of 8-scene chlorophyll-a concentration data in the day of September 13, 2015. In the whole Bohai sea area except the Bohai Strait, the standard deviation of the chlorophyll-a value observed in 8-scenes during the day is about 0.5 ug/L, and it can even reach 1.0 ug/l or more in the coastal waters. Fig. 4(b) shows the comparison of chlorophyll-a concentration retrieval results between GOCI single-scene observation data (UTC 04:16) and averaged 8-scene observation data on September 13, 2015 according the cross-section at 38.5°N. We found that the difference between the two can be up to ~2 ug/l (Fig. 4(b)). Those results indicate that the daily chlorophyll-a concentration monitoring results obtained from the frequency of single-scene per day cannot effectively characterize the daily average chlorophyll-a concentration in a specific region. Then, whether the results of analyzing the long-term spatio-temporal variation of chlorophyll-a concentration by using single-scene data per day or 8-scene data per day will also be different? In this study, we compared the results of chlorophyll-a concentration in the total Bohai Sea (37-41°N and 117-122°E) between the two observation frequencies on the monthly and yearly scales, and a detailed quantitative analysis of the differences was performed (Fig. 5). The results show that the monthly average chlorophyll-a concentration based on the daily single-scene data from GOCI over the past decade (blue line in Fig. 5) differs significantly in some months from the monthly average chlorophyll-a concentration obtained from the daily 8-scene imaging data from GOCI (red line in Fig. 5), with the difference values ranging from -0.66 ug/l to 1.49 ug/l (black line in Fig. 5). The largest difference in chlorophyll-a concentration between the two occurred in December 2016, reaching 1.49 ug/l, followed by December 2019 and then December 2014. The annual difference between 2012 and 2020 in chlorophyll-a concentration based on the two is faint and much less than the monthly average (purple and green lines in Fig. 5). Though the yearly change trends of chlorophyll-a concentration over the decade are generally consistant based on the two data (single-scene versus eight-scene daily average observations), the chlorophyll-a concentration values are varies from each other, and even the results of short-term changes are inconsistent. For example, there is a decreasing trend from 2014 to 2017, and an increasing trend from 2019 to 2020 based on GOCI daily single-scene imaging data (purple line in Fig. 5), which is consistent with previously published trends by using MODIS. However, the annual variation trend of chlorophyll-a concentration based on GOCI daily 8-scene imaging data shows a more gradual change from 2014 to 2017 (green line in Fig. 5). Actually this difference is understandable, because the single-scene GOCI data is acquired at 04:16 (UTC), according to the results of CHLA daily variation (Fig. 3), this is the moment when CHLA concentration is higher, and the average value of GOCI 8 data from morning to night will effectively change the mean result of selecting only higher CHLA concentration value, which is caused by the different data

sources we use. The subsequent analysis of the spatial-temporal variation process of chlorophyll-a concentration in the Bohai Sea will use data obtained from GOCI's daily 8-scene imaging data.

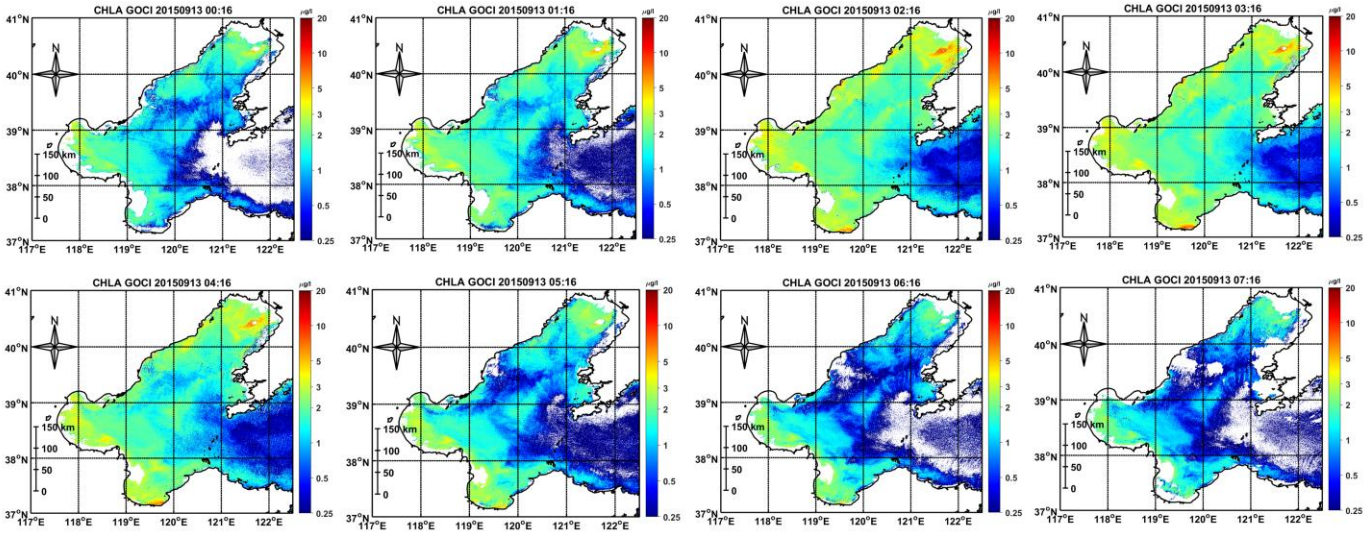

Fig. 3. Eight spatial distribution figures of chlorophyll-a concentration monitored by GOCI on September 13, 2015.

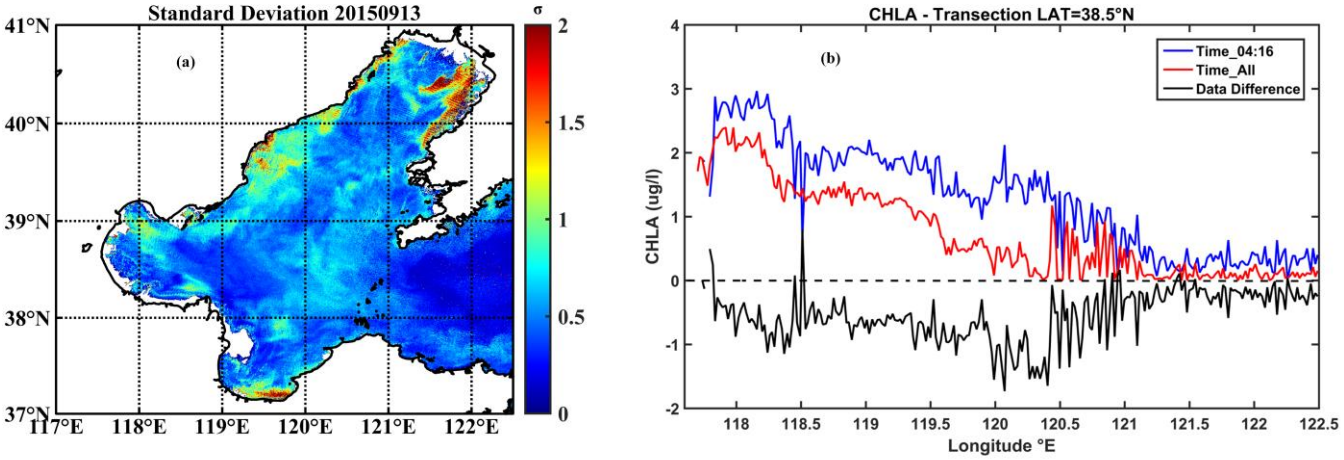

Fig. 4. (a) Standard deviation distribution of 8-scene chlorophyll-a concentration data in one day of September 13, 2015. (b) Comparison of chlorophyll-a concentration changes along 38.5°N cross-section, the blue line is the chlorophyll-a concentration value retrieved from the GOCI single-scene imaging data (04:16 UTC); the red line is the mean value of chlorophyll-a concentration retrieved by GOCI imaging data from 8-scene throughout the day; the black line is the difference results of the two. Data Difference =CHLA_Time_all - CHLA_Time_04.

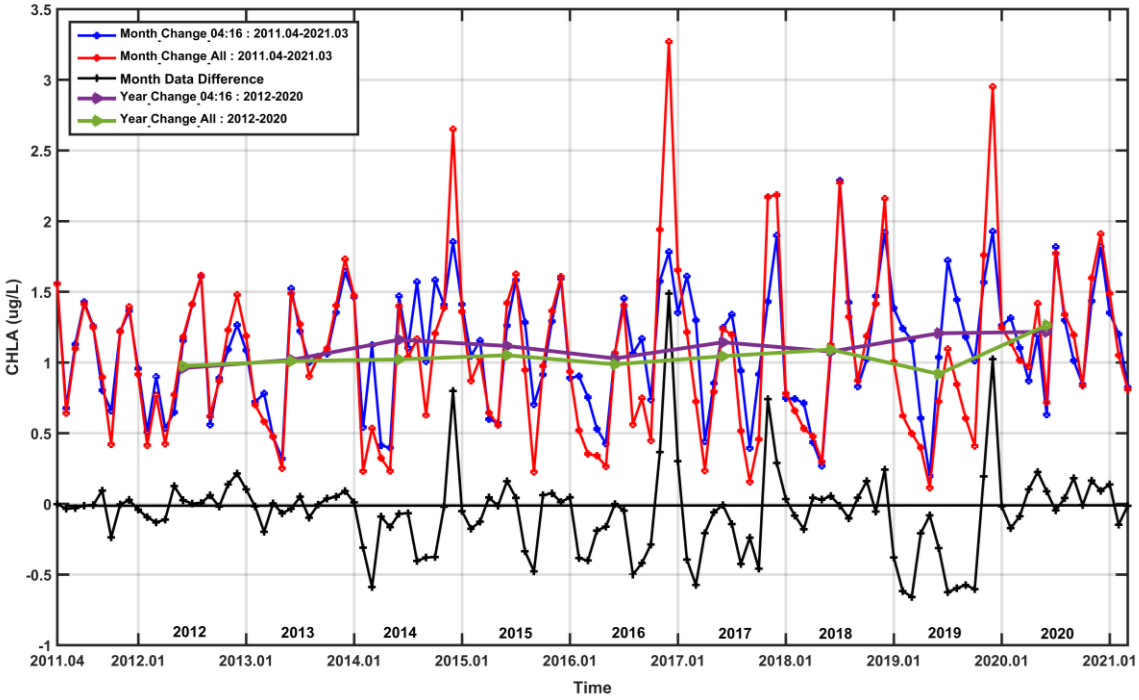

Fig. 5. Monthly and yearly average data of chlorophyll-a concentration in Bohai Sea monitored by GOCI (a) Blue line: monthly mean chlorophyll-a concentration obtained based on the daily single-scene GOCI imaging data (04:16 UTC); (b) Red line: monthly mean chlorophyll-a concentration obtained based on the daily 8-scene GOCI imaging data; (c) Black line: the difference between the above two (Month Data Difference=Month_CHLA_Time_all - Month_CHLA_Time_04). (d) Purple line: annual mean chlorophyll-a concentration obtained based on the daily single-scene GOCI imaging data (04:16 UTC); (e) Green line: annual mean chlorophyll-a concentration obtained based on the daily 8-scene GOCI imaging data.

C. Spatial and temporal distribution of CHLA in Bohai Sea

In this paper, chlorophyll-a concentration data in Bohai Sea were retrieved based on the GOCI data from April 2011 to March 2020, and the monthly mean spatial distribution results for the decade were obtained (Fig. 6). Each line from top to bottom in Fig. 6 represents the four seasons of spring (March, April, May), summer (June, July, August), autumn (September, October, November) and winter (December, January, February). We can find that the chlorophyll-a concentration in spring and autumn were lower than that in summer and winter. The high chlorophyll-a in summer can be explained that higher sea surface temperatures encourage the growth of phytoplankton. The high chlorophyll-a in winter can be explained that strong winter winds and lower sea surface temperature enhance vertical mixing and nutrients from subsurface layers brought to the euphotic layer. The results also show that the chlorophyll-a concentration value increases gradually from deep water to shallow water, with a general distribution trend of high near shore and low far shore. The concentration of chlorophyll-a in the Bohai Strait is the lowest, and the concentration of chlorophyll-a in the central of the Bohai Sea area is lower than that in the other three bays.

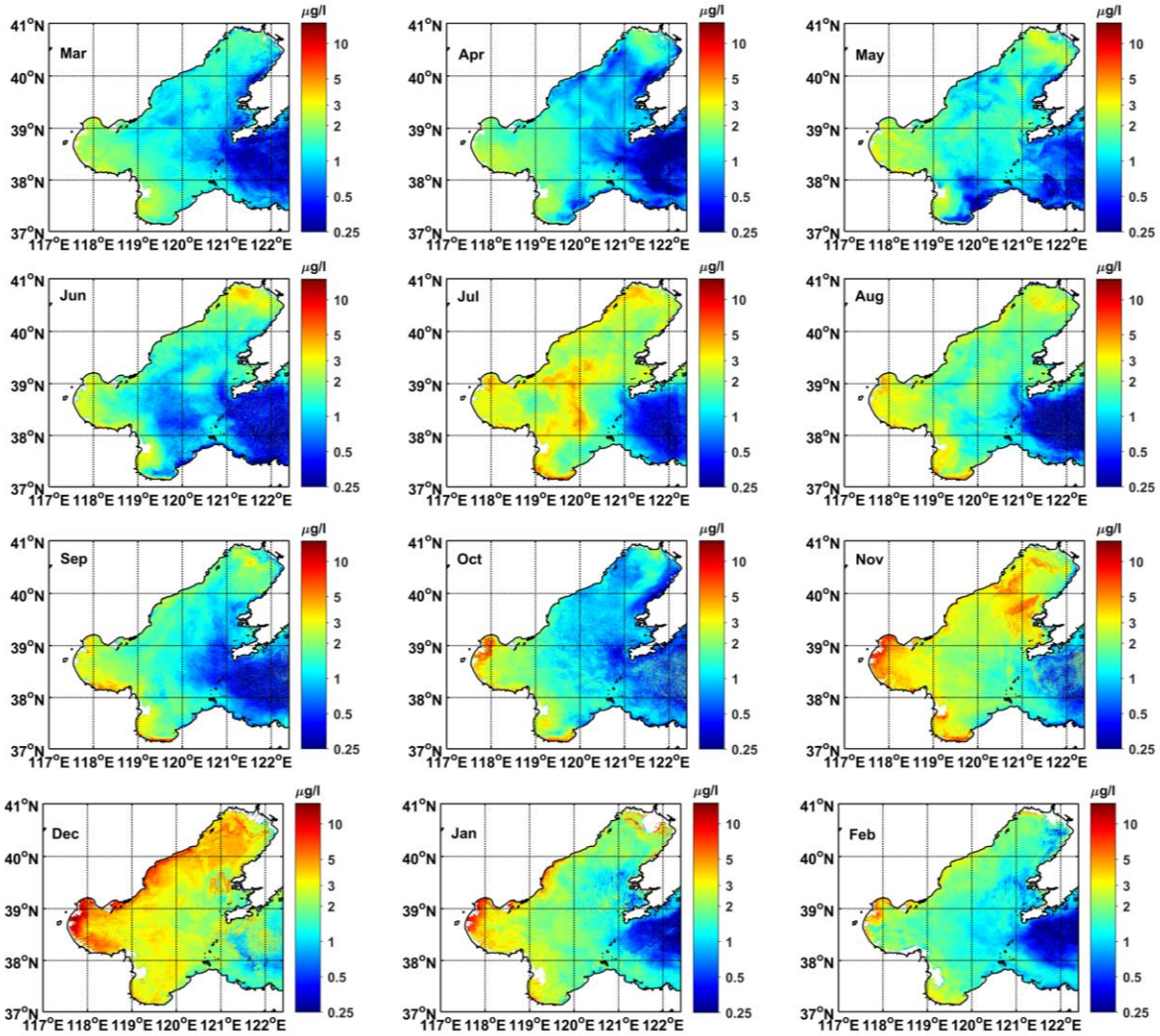

Fig. 6. Monthly average data results of GOCI monitoring of chlorophyll-a concentration in Bohai Sea from April 2011 to March 2020 over the decade. Each line from top to bottom represents the four seasons of spring, summer, autumn and winter.

To better analyze the spatial-temporal variations, this study provides annual average concentration change lines for the Central Bohai Sea, three bay areas, and the Bohai Strait from 2012 to 2020 (Fig. 7). It was observed that the annual average concentration of chlorophyll-a in the Bohai Bay region (black line in Fig. 7) was significantly higher than in other areas of the Bohai Sea, while the concentration in the Bohai Strait (green line in Fig. 7) was significantly lower than in other Bohai Sea regions. During the period from 2012 to 2020, the chlorophyll-a concentration in the Bohai Bay region exhibited a noticeable increasing trend, while the concentrations in Laizhou Bay and Liaodong Bay showed relatively small annual variations, maintaining an average around 1.5 ug/l. Except for the year 2020, the Central Bohai Sea region exhibited a relatively stable annual average chlorophyll-a concentration from 2012 to 2019, consistently around 1.15 ug/l. In the Bohai Strait, the annual average chlorophyll-a concentration remained below 0.5 ug/l. Furthermore, it is noteworthy that, except for the Bohai Strait in 2020, the chlorophyll-a concentrations in other Bohai Sea regions reached their highest levels in nearly a decade.

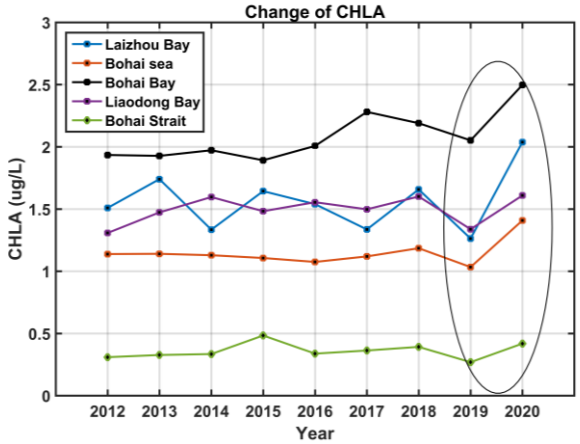

Fig. 7. Results of interannual variation of chlorophyll-a concentration in different regions of the Bohai Sea during 2012-2020.

D. The change of CHLA in Bohai Sea during COVID-19 Lockdown

At the end of 2019, the COVID-19 broke out in China, which had varying degrees of impact on human activities both nationwide and globally for a long period of time thereafter. From January 23 to April 8, 2020, Wuhan, Hubei Province, was under a "lockdown" period, and many other regions in China, including cities along the Bohai Sea, implemented numerous epidemic prevention policies. This pandemic had a significant impact on people's daily lives and also resulted in reduced coastal activities and a slowdown in the development of the marine fisheries economy, which in turn had a considerable impact on the marine ecosystem. In this study, we analyzed the changes in chlorophyll a concentration in the Bohai Sea before and after the COVID-19 outbreak using monthly average data from 2015 to 2020 (Fig. 8 and Fig. 9). It is important to note that we are only presenting the change facts of chlorophyll-a concentration during the COVID-19 period, which does not necessarily imply that the variations of chlorophyll-a concentration during this time were caused by the lockdown due to COVID-19.

The results show that the chlorophyll-a concentration in Bohai Sea during the strictest period (February to April in 2020) of COVID-19 control measures in 2020 (black line in Fig. 8) was significantly higher than the same period of the previous year (2019, green line in Fig. 8), and also higher than the average level during the same period from 2015-2019 (red line in Fig. 8). With the end of the lockdown in Wuhan in April, the relaxation of the national epidemic prevention policy, the increase of industrial activities in cities around the Bohai Sea, and the orderly resumption of production and work, the chlorophyll-a concentration in Bohai Sea showed a rapid rising trend from April to May 2020, with an increase over 0.4 ug/l. In contrast to the upward trend in chlorophyll-a concentration during the same period from May to July in 2015-2019, the chlorophyll-a concentration in the Bohai Sea in May-July 2020 showed a different pattern, with a rapid decrease (decrease of over 0.7 ug/L) followed by a rapid increase (increase of over 1.0 ug/L). The chlorophyll a concentration in the Bohai Sea reached its lowest value in June 2020, deviating significantly from the previous months with the lowest chlorophyll-a concentration in the Bohai Sea (May or September). The anomaly change of monthly chlorophyll-a concentration shows a significant increasing trend from January to May in 2020 (Fig. 9).

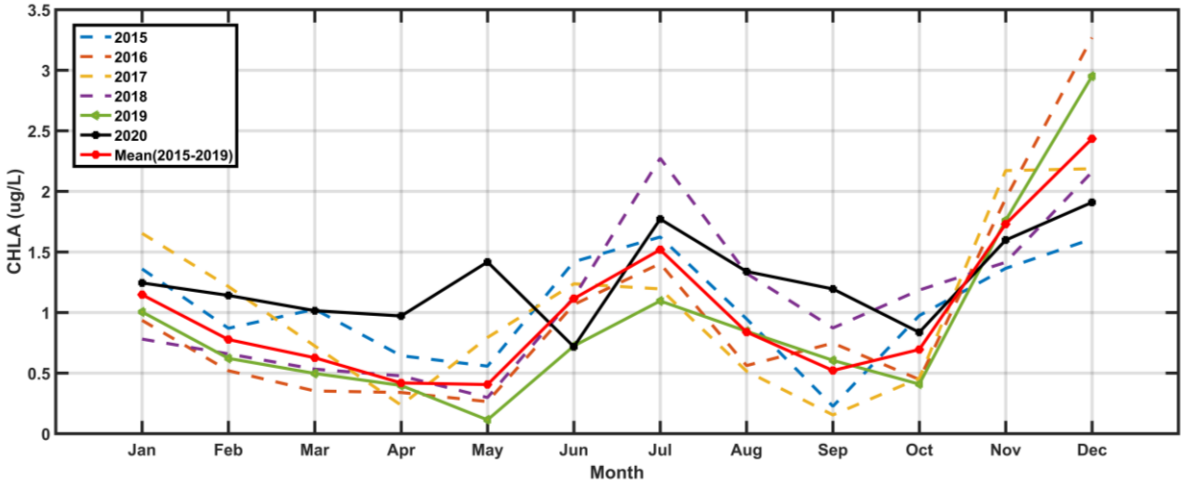

Fig. 8. Comparison diagram of monthly mean chlorophyll-a concentration changes in Bohai Sea from 2015 to 2020

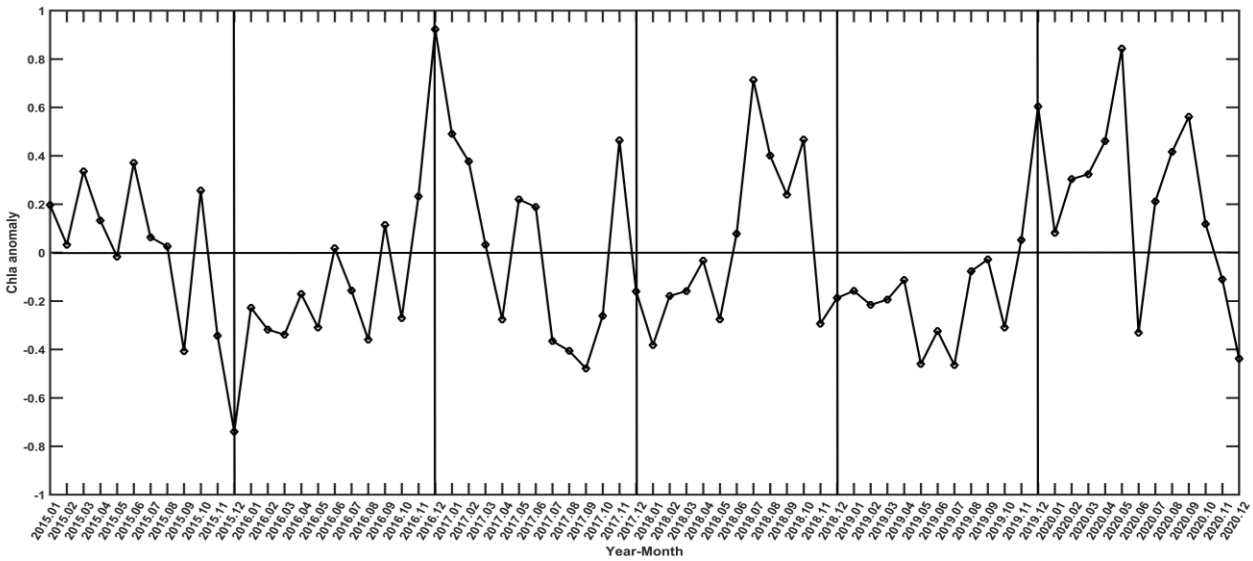

Fig. 9. The anomaly change of chlorophyll-a concentration in Bohai Sea from January 2015 to December 2020

V. Discussion

A. The uncertainty in the assessment of CHLA retrieval performance

Due to the limited amount of in-situ measured chlorophyll-a concentration data, there are still some uncertainties and limitations in evaluating the results of this study. Firstly, these uncertainties may arise from the less stringent spatio-temporal matching criteria between the satellite and in-situ chlorophyll-a concentration data. Generally, a time window of ±3hours should be set to obtain the matching pairs between the satellite data and the measured data [64]. However, in this study, we set the time window to ±5 hours in order to obtain a sufficient number of matching data. In future studies, more in-situ chlorophyll-a data need to be further acquired, and the time matching window should be strictly controlled within ±3hours. Secondly, the selection of atmospheric correction algorithms and chlorophyll-a concentration retrieval models were limited. In this study, only four atmospheric correction algorithms and four chlorophyll a concentration retrieval models were used. In future research, other atmospheric correction algorithms, such as those based on artificial neural network algorithms[65], and other chlorophyll a concentration retrieval models, such as the GAM (generalized additive model) proposed by Wang et al. [62, 66], can be attempted to further improve the comparative results of this study.

B. Reliability of GOCI data in Marine ecological monitoring

The GOCI satellite sensor data used in this paper can provide 8-scene observation data from 8 a.m. to 15 p.m. of the Beijing local time every day. Compared with the traditional polar-orbiting satellite sensor which can only provide single-scene observation data per day (such as MODIS), its data sampling frequency was increased by 8 times, and the effective data coverage rate of daily average monitoring data was also significantly improved. GOCI has irreplaceable advantages in monitoring short-term and long-term changes of Marine ecological parameters. The results of this paper show that there are differences between the monitoring results of chlorophyll-a concentration based on 8-scene of GOCI data and that based on single view of GOCI data (equivalent to the traditional polar satellite sensor data) in the comparison of daily mean (Fig. 4), monthly mean and annual mean (Fig. 5). Although many Studies have also mentioned the advantages of GOCI monitoring Marine ecological environment, most of them focus on the analysis of its hourly changes [42, 67], and there is no clear quantitative analysis of the differences between GOCI multi-scene sampling data and single-scene sampling data as in this study. The results of this study indicate that early conclusions on the temporal-spatial changes of Marine ecological parameters (such as chlorophyll-a concentration) based on traditional low-sampling frequency polar-orbiting satellite data should be treated with caution [9, 68]. Although the high-frequency sampling frequency of GOCI has partially improved the effective coverage of daily monitoring data in the target sea area, the effective data coverage of GOCI satellite is still insufficient due to the influence of clouds, fog, solar flares and thick aerosols, and these missing data will seriously affect the spatio-temporal continuity of water color remote sensing products. It even has a certain impact on the related research results of spatio-temporal changes. In the next research, it is still necessary to consider developing a data reconstruction algorithm that suitable for GOCI high-frequency sampling characteristics to further perfect the research results of this paper. In addition, some reports have raised doubts about the usability of dawn and dusk monitoring data obtained by GOCI sensors, although results of the study by QIAO et al. [69] show that the quality of the GOCI dawn and dusk monitoring data is reliable at 412-680nm. But the amount of in-situ measured chlorophyll a concentration data obtained in this study is limited. There aren't sufficient conditions to evaluate the chlorophyll-a concentration products retrieved from the morning and evening monitoring data of GOCI. This remains one of the aspects that needs further improvement in subsequent research.

One of the purposes of this manuscript is to encourage research groups that own a lot of field data to supplement the analysis of this part.

C. The CHLA in the different areas of Bohai Sea

From 2012 to 2020, the chlorophyll-a in the Bohai Strait were in a low state for a long time. The reason may be that the Bohai Strait is the channel connecting the Bohai Sea and the Yellow Sea, and a large amount of salt water in the Yellow Sea flows into it, so the water environment is very unfavorable for the growth of phytoplankton [44]. The Central Bohai Sea area is far from the land, and the impact of human activities in this area is lower than that in the three Bays. Moreover, the high-concentration salt water exchanged from the Yellow Sea through the Bohai Strait also affects the stability of the environment in this area, which is not conducive to the aggregation of phytoplankton. Therefore, the concentration of chlorophyll-a in this area is higher than that in the Bohai Strait but lower than that in the Bohai Bay, Laizhou Bay and Liaodong Bay. The Bohai Bay, Laizhou Bay and Liaodong Bay are surrounded by the Bohai economic circle with a high degree of industrialization and a relatively dense population, and they are also the main receiving areas for a large number of rivers, such as the Yellow River flowing into Laizhou Bay, the Liaohe River flowing into Liaodong Bay, and the Luanhe River flowing into the northern area of Bohai Bay [70]. Extensive mariculture areas are situated on both sides of the estuary, and high chlorophyll-a concentration appears in the three bays due to the substantial nutrient discharge directly into the bays. In particular, Bohai Bay is the hub of shipping in North China. It is surrounded by land on three sides and adjacent to the land of Hebei, Tianjin and Shandong. We suspect that the prosperous industrial production and other activities along the coast lead to a significant increase in the amount of nutrients discharged into Bohai Bay, which in turn promotes algae reproduction, resulting in a higher concentration of chlorophyll a in the water body than in the other two bays [44]. So a variety of reasons lead to the spatio-temporal variability of CHLA in areas of the Bohai Sea are not completely consistent (Fig. 7 and Fig. 8).

D. Uncertainty of factors for drastic change of CHLA in Bohai Sea in 2020

The detailed changes of chlorophyll-a concentration in Bohai Sea before and after Covid-19 are given in Section IV.D of this paper. And compared with the same period level in 2019 or the same period average in 2015-2019, the chlorophyll-a concentration in more than 92% of the whole sea areas was significantly increased in the period from January to May of 2020, when the epidemic prevention and control period was relatively strict (Fig. 10). The lockdown and restriction measures implemented by coastal cities around the Bohai Sea during Covid-19 (Table 2) [71] have alleviated the pressure of human activities on Marine ecology, which is possible one of the reasons for this change. However, previous studies have shown that chlorophyll-a concentration is not only affected by human activities, but also by natural factors such as precipitation, wind speed, sea surface temperature, nutrient salts, etc. [72]. Therefore, the cause of drastic changes in chlorophyll-a concentration in Bohai Sea in 2020 should be analyzed by combining the dual factors of natural environment and human activities to better quantify the proportion of each influencing factor. Here, we applied the GMI monthly average rain rate, sea surface temperature and wind speed data from 2015 to 2020 to analyze the causes of the changes (Fig. 11). We can find that the average rain rate in 2019 was about 0.15mm/h, which is significantly lower than the 0.42mm/h in 2018. The average wind speed in 2019 also decreased to 5.1m/s from 5.3m/s in 2018. The sea surface temperature in 2019 did not change significantly, only changing from 14.6°C in 2018 to 14.9°C. Therefore, the decrease of chlorophyll-a concentration in Bohai Sea in 2019 can be attributed to the decrease of runoff caused by the decrease of rainfall, thus reducing the input of terrestrial nutrients into the ocean. At the same time, the small decrease of wind speed more or less weakens the water mixing, which affects the vertical transport of nutrients from the depth of the water and inhibits the growth of phytoplankton. However, in 2020, the mean wind speed continued to decrease to 5.0m/s, the mean rainfall was about 0.18mm/h, the mean sea surface temperature was about 15.0°which were not much higher than that in 2019. If the impact of human activities was not considered, convincing explanation should be that changes in these natural factors will not lead to drastic changes in the concentration of chlorophyll a in the Bohai Sea in 2020. However, the results of this study show that the average concentration of chlorophyll a in Bohai Sea in 2020 has reached the highest value in this decade. Therefore, we infer that the unusually high value of chlorophyll a concentration in the Bohai Sea in 2020 has a high probability to be related to the abnormal human activities during COVID-19. However, it is worth noting that the resolution of GMI data is low, which may affect the certainty of the analysis results. The conclusions of this part of the study need to be supplemented with more data on other nutrients, such as nitrogen and phosphorus.

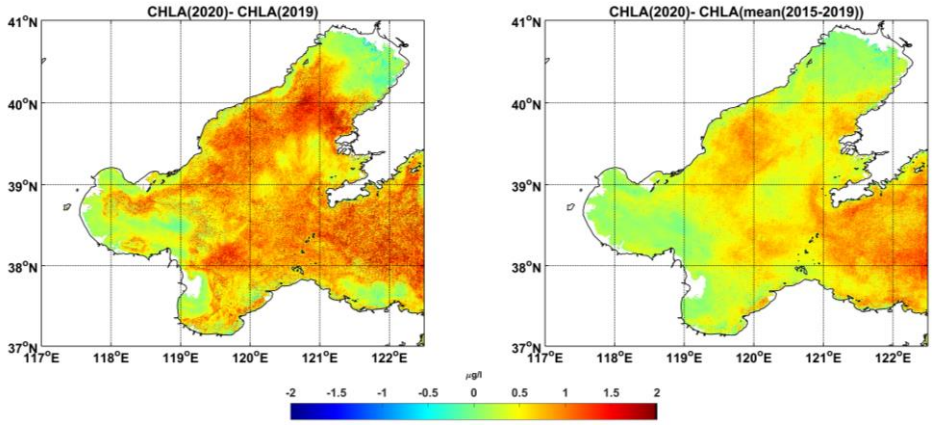

Fig. 10. The difference value of average chlorophyll-a concentration in Bohai Sea from January to May in 2020 compared with the same period in 2019 (left), and compared with the same period in 2015-2019 (right)

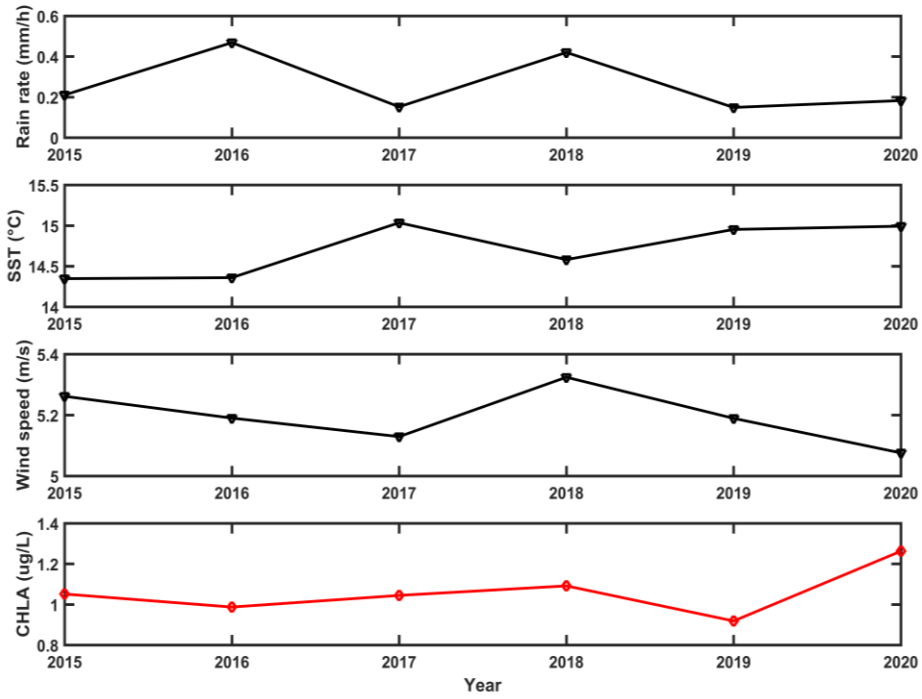

Fig. 11 The yearly changes of rain rate, sea surface temperature, wind speed and chlorophyll-a concentration in Bohai Sea from 2015 to 2020

TABLE 2 CITIES AND START TIMES OF COVID-19 LOCKDOWN POLICIES IN BOHAI RIM

City	Start time
Qin huang dao	2022.01.25
Tang shan	2022.01.28
Dong ying	2022.01.30
Hu lu dao	2022.02.05
Jin zhou	2022.02.05
Pan Jin	2022.02.05
Da Lian	2022.02.05
Tian jin	2022.02.06
Cang zhou	2022.02.09

VI. Conclusion

The adaptability of four chlorophyll-a concentration retrieval models (OC2, YOC, OC3G, OC2M-HI) under four atmospheric correction algorithms (GDPS1.4.1, GDPS2.0, Seadas Default, and Seadas MUMM) in the Bohai Sea were evaluated based on in-situ chlorophyll-a concentration data. And a clear quantitative analysis was conducted on the differences in the spatial-temporal distribution of chlorophyll-a concentration in the Bohai Sea monitored by GOCI based on 8-scene sampling data and single scene sampling data (which can be seen similar to the results of traditional polar-orbiting satellite data). The results of this study indicate that the differences in chlorophyll-a concentration values caused by different atmospheric correction algorithms cannot be ignored. It is not recommended to use OC2 and OC3G chlorophyll-a concentration retrieval models in the Bohai Sea. To obtain chlorophyll-a concentration data products with high retrieval accuracy, both atmospheric correction algorithms and chlorophyll-a concentration retrieval models need to be considered simultaneously, and the best combination of the two should be selected. The comparison with in-situ CHLA data shows that the combination of atmospheric correction algorithms based on Seadas_Default or Seadas_MUMM and YOC chlorophyll-a concentration retrieval model is more suitable for GOCI data to retrieve chlorophyll-a concentration in the Bohai Sea. At the same time, the research results of this paper also suggest that we should be cautious about the conclusions obtained from early researches on the spatial-temporal changes of marine ecological parameters (such as chlorophyll-a concentration) based on traditional polar-orbiting satellite data with low sampling frequency.

Acknowledgment

We would like to thank the KOSC for providing GOCI data and various versions of GDPS software. And we also gratitude to NASA Ocean Biology Processing Group for providing SeaDAS software.

References

[1] X. Gao, F. Zhou, and C. T. Chen, "Pollution status of the Bohai Sea: an overview of the environmental quality assessment related trace metals," *Environ. Int.*, vol. 62, pp. 12-30, Jan 2014. doi: 10.1016/j.envint.2013.09.019

[2] S. Liu *et al.*, "Water quality assessment by pollution-index method in the coastal waters of Hebei Province in western Bohai Sea, China," *Mar. Pollut. Bull.*, vol. 62, no. 10, pp. 2220-9, Oct 2011. doi: 10.1016/j.marpolbul.2011.06.021

[3] X. Ning *et al.*, "Long-term environmental changes and the responses of the ecosystems in the Bohai Sea during 1960–1996," *DEEP-SEA RES PT II*, vol. 57, no. 11-12, pp. 1079-1091, 2010. doi: 10.1016/j.dsr2.2010.02.010

[4] Q. Tang, X. Jin, J. Wang, Z. Zhuang, Y. Cui, and T. Meng, "Decadal-scale variations of ecosystem productivity and control mechanisms in the Bohai Sea," *Fish. Oceanogr.*, vol. 12, no. 4-5, pp. 223-233, 2003. doi: 10.1046/j.1365-2419.2003.00251.x

[5] P. Kasprzak, J. Padisák, R. Koschel, L. Krienitz, and F. Gervais, "Chlorophyll a concentration across a trophic gradient of lakes: An estimator of phytoplankton biomass?," *Limnologica*, vol. 38, no. 3-4, pp. 327-338, 2008. doi: 10.1016/j.limno.2008.07.002

[6] N. Ha, K. Koike, and M. Nhuan, "Improved Accuracy of Chlorophyll-a Concentration Estimates from MODIS Imagery Using a Two-Band Ratio Algorithm and Geostatistics: As Applied to the Monitoring of Eutrophication Processes over Tien Yen Bay (Northern Vietnam)," *Remote Sens.*, vol. 6, no. 1, pp. 421-442, 2013. doi: 10.3390/rs6010421

[7] B. Fründt, J. W. Dippner, and J. J. Waniek, "Chlorophyll a reconstruction from in situ measurements: 1. Method description," *J. Geophys. Res-Biogeo.*, vol. 120, no. 2, pp. 237-245, 2015. doi: 10.1002/2014JG002691

[8] V. V. Povazhnyi, "Determination of the chlorophyll “a” concentration using a combined method based on measurements with a modified photometer.," *Oceanology*, vol. 52, pp. 561–565, 2012. doi: 10.1134/s0001437012040078

[9] M. Xu, R. Liu, J. M. Chen, Y. Liu, and A. Wolanin, "A 21-Year Time Series of Global Leaf Chlorophyll Content Maps From MODIS Imagery," *IEEE Trans. Geosci. Remote Sens.*, vol. 60, pp. 1-13, 2022. doi: 10.1109/TGRS.2022.3204185.

[10] M. Darecki, S. Kaczmarek, and J. Olszewski, "SeaWiFS ocean colour chlorophyll algorithms for the southern Baltic Sea," *Int. J. Remote Sens.*, vol. 26, no. 2, pp. 247-260, 2007. doi: 10.1080/01431160410001720298

[11] L. Sun, M. Guo, and X. Wang, "Ocean color products retrieval and validation around China coast with MODIS," *Acta Oceanol. Sin.*, vol. 29, no. 4, pp. 21-27, 2010. doi: 10.1007/s13131-010-0047-6

[12] W. J. Moses *et al.*, "Estimation of chlorophyll-a concentration in turbid productive waters using airborne hyperspectral data," *Water Res.*, vol. 46, no. 4, pp. 993-1004, Mar 15 2012. doi: 10.1016/j.watres.2011.11.068

[13] C. R. Bostater *et al.*, "Assessment of satellite retrieval algorithms for chlorophyll-a concentration under high solar zenith angle," presented at the Remote Sensing of the Ocean, Sea Ice, Coastal Waters, and Large Water Regions, 2016.

[14] M. R. Al Shehhi, I. Gherboudj, J. Zhao, and H. Ghedira, "Improved atmospheric correction and chlorophyll-a remote sensing models for turbid waters in a dusty environment," *Isprs. J. Photogramm*, vol. 133, pp. 46-60, 2017. doi: 10.1016/j.isprsjprs.2017.09.011

[15] E. S. Pereira and C. A. E. Garcia, "Evaluation of satellite-derived MODIS chlorophyll algorithms in the northern Antarctic Peninsula," *DEEP-SEA RES PT II*, vol. 149, pp. 124-137, 2018. doi: 10.1016/j.dsr2.2017.12.018

[16] G. H. Tilstone *et al.*, "Performance of Ocean Colour Chlorophyll a algorithms for Sentinel-3 OLCI, MODIS-Aqua and Suomi-VIIRS in open-ocean waters of the Atlantic," *Remote Sens. Environ.*, vol. 260, 2021. doi: 10.1016/j.rse.2021.112444

[17] G. Dall'Olmo, A. A. Gitelson, and D. C. Rundquist, "Towards a unified approach for remote estimation of chlorophyll-a in both terrestrial vegetation and turbid productive waters," *Geophys. Res. Lett.*, vol. 30, no. 18, 2003. doi: 10.1029/2003GL018065

[18] W. J. Moses, A. A. Gitelson, S. Berdnikov, and V. Povazhnyy, "Satellite Estimation of Chlorophyll-a Concentration Using the Red and NIR Bands of MERIS—The Azov Sea Case Study," *IEEE Geosci. Remote Sens.*, vol. 6, no. 4, pp. 845-849, 2009. doi: 10.1109/lgrs.2009.2026657

[19] C. Hu, Z. Lee, and B. Franz, "Chlorophyll aalgorithms for oligotrophic oceans: A novel approach based on three-band reflectance difference," *J. Geophys. Res-Oceans.*, vol. 117, no. C1, 2012. doi: 10.1029/2011JC007395

[20] S. Mishra and D. R. Mishra, "Normalized difference chlorophyll index: A novel model for remote estimation of chlorophyll-a concentration in turbid productive waters," *Remote Sens. Environ.*, vol. 117, pp. 394-406, 2012. doi: 10.1016/j.rse.2011.10.016

[21] W. Yang, B. Matsushita, J. Chen, T. Fukushima, and R. Ma, "An enhanced three-band index for estimating chlorophyll-a in turbid case-II waters: case studies of Lake Kasumigaura, Japan, and Lake Dianchi, China," *IEEE Geosci. Remote S.*, vol. 7, no. 4, pp. 655-659, 2010. doi: 10.1109/LGRS.2010.2044364

[22] J. Gower, "Observations of in situ fluorescence of chlorophyll-a in Saanich Inlet," *Bound-Lay. Meteorol.*, vol. 18, no. 3, pp. 235-245, 1980. doi: 10.1007/BF00122022

[23] K. A. Ali and W. J. Moses, "Application of a PLS-Augmented ANN Model for Retrieving Chlorophyll-a from Hyperspectral Data in Case 2 Waters of the Western Basin of Lake Erie," *Remote Sens.*, vol. 14, no. 15, 2022. doi: 10.3390/rs14153729

[24] J. Luo *et al.*, "Research progress in the retrieval algorithms for chlorophyll-a, a key element of water quality monitoring by remote

sensing," *Remote Sensing Technology and Application*, vol. 36, no. 3, pp. 473-488, 2021. doi: 10.11873/j.issn.1004-0323.2021.3.0473

[25] X. Li, J. Sha, and Z.-L. Wang, "Application of feature selection and regression models for chlorophyll-a prediction in a shallow lake," *Environ. Sci. Pollut. R.*, vol. 25, pp. 19488-19498, 2018. doi: 10.1007/s11356-018-2147-3

[26] H. S. B and M. C. R, "The calibration and validation of SeaWIFS data," *Prog. Oceanogr.*, vol. 45, no. 3, pp. 427-465, 2000. doi: 10.1016/s0079-6611(00)00012-4

[27] S. Guo *et al.*, "MODIS ocean color product downscaling via spatio-temporal fusion and regression: The case of chlorophyll-a in coastal waters," *Int. J. Appl. Earth Obs.*, vol. 73, pp. 340-361, 2018. doi: 10.1016/j.jag.2018.06.004

[28] E. Siswanto *et al.*, "Empirical ocean-color algorithms to retrieve chlorophyll-a, total suspended matter, and colored dissolved organic matter absorption coefficient in the Yellow and East China Seas," *J. Oceanogr.*, vol. 67, no. 5, pp. 627-650, 2011. doi: 10.1007/s10872-011-0062-z

[29] G. Dall'Olmo, A. A. Gitelson, D. C. Rundquist, B. Leavitt, T. Barrow, and J. C. Holz, "Assessing the potential of SeaWiFS and MODIS for estimating chlorophyll concentration in turbid productive waters using red and near-infrared bands," *Remote Sens. Environ.*, vol. 96, no. 2, pp. 176-187, 2005. doi: 10.1016/j.rse.2005.02.007

[30] Z. Lee, K. L. Carder, and R. A. Arnone, "Deriving inherent optical properties from water color: A multi-band quasi-analytical algorithm for optically deep waters," *Appl. Opt.*, vol. 41, no. 27, pp. 5755-5772, 2002. doi: 10.1364/AO.41.005755

[31] J. Wei and Z. P. Lee, "Retrieval of phytoplankton and color detrital matter absorption coefficients with remote sensing reflectance in an ultraviolet band," *Appl. Opt.*, vol. 54(4), pp. 636–649, 2015. doi: 10.1364/ao.54.000636

[32] X. He, Y. Bai, D. Pan, J. Tang, and D. Wang, "Atmospheric correction of satellite ocean color imagery using the ultraviolet wavelength for highly turbid waters," *Opt. Express*, vol. 20, no. 18, pp. 20754-20770, 2012. doi: 10.1364/OE.20.020754

[33] M. Wang and W. Shi, "Remote Sensing of the Ocean Contributions from Ultraviolet to Near-Infrared Using the ShortwaveInfrared Bands: Simulations," *Appl. Opt.*, vol. 46, no. 9, pp. 1535-1547, 2007. doi: 10.1364/AO.46.001535

[34] G. F. Moore, J. Aiken, and S. J. Lavender, "The atmospheric correction of water colour and the quantitative retrieval of suspended particulate matter in Case II waters: Application to MERIS," *Int. J. Remote Sens.*, vol. 20, no. 9, pp. 1713-1733, 1999. doi: 10.1080/014311699212434

[35] J.-H. Ahn, Y.-J. Park, J.-H. Ryu, B. Lee, and I. S. Oh, "Development of atmospheric correction algorithm for Geostationary Ocean Color Imager （GOCI）," *Ocean. Sci. J.*, vol. 47, no. 3, pp. 247-259, 2012. doi: 10.1007/s12601-012-0026-2

[36] C. Jamet, S. Thiria, and C. Moulin, "Use of a Neurovariational Inversion for Retrieving Oceanic and Atmospheric Constituents from Ocean Color Imagery: A Feasibility Study," *J. Atmos. Ocean. Tech.* , vol. 22, pp. 460-475, 2005. doi: 10.1175/JTECH1688.1

[37] T. Schroeder, I. Behnert, M. Schaale, J. Fischer, and R. Doerffer, "Atmospheric correction algorithm for MERIS above case-2 waters," *J. Remote Sens.* , vol. 28, pp. 1469–1486, 2007. doi: 10.1080/01431160600962574

[38] J. Brajard, R. Santer, M. Crpon, and S. Thiria, "Atmospheric correction of MERIS data for case-2 waters using a neuro-variational inversion," *Remote Sens. Environ.*, vol. 126, pp. 51-61, 2012. doi: 10.1016/j.rse.2012.07.004

[39] J. Brajard, C. Jamet, S. Thiria, C. Moulin, and M. Crepon, "Use of a neuro-variational inversion for retrieving oceanic and atmospheric constituents from satellite ocean color sensor: Application to absorbing aerosols," *Neural Netw.*, vol. 22, pp. 460-475, 2006. doi: 10.1016/j.neunet.2006.01.015

[40] C. P. Kuchinke, H. R. Gordon, L. W. Harding, and K. J. Voss, "Spectral optimization for constituent retrieval in Case II waters II: Validation study in the Chesapeake Bay," *Remote Sens. Environ.* , vol. 113, pp. 610-621, 2009. doi: 10.1016/j.rse.2008.11.002

[41] R. Chomko, H. Gordon, S. Maritorena, and D. Siegel, "Simultaneous retrieval of oceanic and atmospheric parameters for ocean color imagery by spectral optimization: a validation," *Remote Sens. Environ.*, vol. 84, no. 2, pp. 208-220, 2003. doi: 10.1016/S0034-4257(02)00108-6

[42] X. Liu, Q. Yang, Y. Wang, and Y. Zhang, "Evaluation of GOCI Remote Sensing Reflectance Spectral Quality Based on a Quality Assurance Score System in the Bohai Sea," *Remote Sens.*, vol. 14, no. 5, 2022. doi: 10.3390/rs14051075

[43] F. Zhai, W. Wu, Y. Gu, P. Li, X. Song, and P. Liu, "Interannual-decadal variation in satellite-derived surface chlorophyll-a concentration in the Bohai Sea over the past 16 years," *J. Marine Syst.*, vol. 215, p. 103496, 2021. doi: 10.1016/j.jmarsys.2020.103496

[44] Y. Du, X. Zhang, S. Ma, and N. Yao, "Chlorophyll-a concentration variations in Bohai sea: Impacts of environmental complexity and human activities based on remote sensing technologies," *Big Data Res.*, vol. 36, p. 100440, 2024. doi: 10.1016/j.bdr.2024.100440

[45] X.-Y. Liu *et al.*, "Comparative Study on Transparency Retrieved From GOCI Under Four Different Atmospheric Correction Algorithms in Jiaozhou Bay and Qingdao Coastal Area," *IEEE J-STARS*, vol. 17, pp. 2077-2089, 2024. doi: 10.1109/JSTARS.2023.3343572

[46] R. Liu, J. Zhang, H. Yao, T. Cui, N. Wang, and Y. Zhang, "Hourly changes in sea surface salinity in coastal waters recorded by Geostationary Ocean Color Imager," *Estuar. Coast. Shelf. S.*, vol. 196, pp. 227-236, 2017. doi: 10.1016/j.ecss.2017.07.004

[47] L. Sun, J. Jiang, and W. Zhu, "Remote sensing inversion and daily variation of CDOM based on GOCI in the Changjiang Estuary and adjacent waters," *Haiyang Xuebao*, vol. 39, no. 9, pp. 133-145, 2017. doi: 10.3969/j.issn.0253-4193.2017.09.013

[48] J. Wang, J. Tang, W. Wang, Y. Wang, and Z. Wang, "Quantitative Retrieval of Chlorophyll-a Concentrations in the Bohai–Yellow Sea Using GOCI Surface Reflectance Products," *Remote Sens.*, p. 5285, 2023. doi: 10.3390/rs15225285

[49] Y. Qian *et al.*, "Evaluation of ocean color products from Korean Geostationary Ocean Color Imager (GOCI) in Jiaozhou Bay and Qingdao coastal area," presented at the International Society for Optics and Photonics, Beijing China, 2014.

[50] W. M. Kim, J.; Park, Y.; Ishizaka, J., "Evalution of chlorophyll retrievals from Geostationary Ocean color Imager (GOCI) for the North-East Asian region," *Remote Sens. Environ.*, vol. 184, pp. 482–495, 2016. doi: 10.1016/j.rse.2016.07.031

[51] J.-H. Ahn, Y.-J. Park, and H. Fukushima, "Comparison of Aerosol Reflectance Correction Schemes Using Two Near-Infrared Wavelengths for Ocean Color Data Processing," *Remote Sens.*, vol. 10, p. 1791, 2018. doi: 10.3390/rs10111791

[52] J.-H. Ryu, H.-J. Han, S. Cho, Y.-J. Park, and Y.-H. Ahn, "Overview of geostationary ocean color imager (GOCI) and GOCI data processing system (GDPS)," *Ocean. Sci. J.*, vol. 47, no. 3, pp. 223-233, 2012. doi: 10.1007/s12601-012-0024-4

[53] J. H. Ahn, Y. J. Park, W. Kim, and B. Lee, "Vicarious calibration of the geostationary ocean color imager," *Opt. Express*, vol. 23, no. 18, pp. 23236-23258, 2015. doi: 10.1364/OE.23.023236

[54] J.-H. AHN, Y.-J. PARK, W. KIM, and B. LEE, "Simple aerosol correction technique based on the spectral relationships of the aerosol multiple-scattering reflectances for atmospheric correction over the oceans," *Opt. Express*, vol. 24, no. 26, pp. 29659-29669, Dec 26 2016. doi: 10.1364/OE.24.029659

[55] H. R. Gordon and M. Wang, "Retrieval of water leaving radiance and aerosol optical thickness over the oceans with SeaWiFS: A preliminary algorithm," *Appl. Opt.*, vol. 33, no. 3, pp. 443-452, 1994. doi: 10.1364/AO.33.000443

[56] R. P. Stumpf, R. A. Arnone, R. W. Gould, P. M. Martinolich, and V. Ransibrahmanakul, "A Partially Coupled Ocean-Atmosphere Model for Retrieval of Water-Leaving Radiance from SeaWiFS in Coastal Waters," *NASA Tech. Memo.*, vol. 22, pp. 51–59, 2003. doi:

[57] S. W. Bailey, B. A. Franz, and P. J. Werdell, "Estimation of near-infraredwater-leaving reflectance for satellite ocean color data processing," *Opt. Express*, vol. 18, no. 7, pp. 7521–7527, 2010. doi: 10.1364/OE.18.007521

[58] Z. Ahmad *et al.*, "New aerosol models for the retrieval of aerosol optical thickness and normalized water-leaving radiances from the SeaWiFS and MODIS sensors over coastal regions and open oceans," *Appl. Opt.*, vol. 49, pp. 5545–5560, 2010. doi: 10.1364/ao.49.005545

[59] K. G. Ruddick, F. Ovidio, and M. Rijkeboer, "Atmospheric correction of SeaWiFS imagery for turbid coastal and inland waters," *Appl. Opt.*, vol. 39, no. 6, pp. 897-912, 2000. doi: 10.1364/AO.39.000897

[60] S. Tassan, "Local algorithms using SeaWiFS data for the retrieval of phytoplankton, pigments, suspended sediment, and yellow substance in coastal waters," *Applied Optics* vol. 33, pp. 2369-2378, 1994. doi:

[61] J. E. O'Reilly, S. Maritorena, B. G. Mitchell, and D. A. Siegel, "Ocean Color Chlorophyll Algorithms for SEAWIFS," *Journal of Geophysical Research: Oceans* vol. 103, no. C11, 1998. doi: 10.1029/98JC02160

[62] M. Wang, J. Tang, and W. Shi, "MODIS-derived Ocean Color Products along the China East Coastal Region," *Geophys. Res. Lett.*, vol. 34, no. 6, 2007. doi: 10.1029/2006gl028599.

[63] D. A. Siegel *et al.*, "Regional to Global Assessments of Phytoplankton Dynamics from the SeaWiFS Mission," *Remote Sens. Environ.*, vol. 135, pp. 77–91, 2013. doi: 10.1016/j.rse.2013.03.025

[64] S. W. Bailey and P. J. Werdell, "A multi-sensor approach for the on-orbit validation of ocean color satellite data products," *Remote Sens. Environ.*, vol. 102, no. 1-2, pp. 12-23, 2006. doi: 10.1016/j.rse.2006.01.015

[65] C. Goyens, C. Jamet, and T. Schroeder, "Evaluation of four atmospheric correction algorithms for MODIS-Aqua images over contrasted coastal waters," *Remote Sens. Environ.*, vol. 131, pp. 63-75, 2013. doi: 10.1016/j.rse.2012.12.006

[66] Y. Wang, D. Liu, Y. Wang, Z. Gao, and J. K. Keesing, "Evaluation of standard and regional satellite chlorophyll-a algorithms for moderate-resolution imaging spectroradiometer (MODIS) in the Bohai and Yellow Seas, China: a comparison of chlorophyll-a magnitude and seasonality," *Int. J. Remote Sens.*, vol. 40, no. 13, pp. 4980-4995, 2019. doi: 10.1080/01431161.2019.1577579

[67] Y. Zhou *et al.*, "Monitoring multi-temporal and spatial variations of water transparency in the Jiaozhou Bay using GOCI data," *Mar. Pollut. Bull.*, vol. 180, p. 113815, Jul 2022. doi: 10.1016/j.marpolbul.2022.113815

[68] K. K. Kivva and A. A. Kubryakov, "Seasonal and Interannual Variability of Chlorophyll-a Concentration in the Bering Sea Found from Satellite Data," *Izv. Atmos. Ocean. Phy+*. vol. 57, no. 12, pp. 1643–1657, 2021. doi: 10.1134/S0001433821120136

[69] Q. Feng, C. Jianyu, and X. Yuying, "Usability Analysis GOCI Twilight Periods Radiative Transfer Model Data," *Marine Information*, vol. 1, pp. 28-39, 2021. doi: 10.19661/j.cnki.mi.2021.01.005

[70] S. Shang, Z. Lee, L. Shi, G. Lin, G. Wei, and X. Li, "Changes in water clarity of the Bohai Sea: Observations fromMODIS," *Remote Sens. Environ.*, vol. 186, pp. 22-31, 2016. doi: 10.1016/j.rse.2016.08.020

[71] X. Xiao, S. Huang, and J. He, "The impact of COVID-19 lockdown on the variation of sea surface chlorophyll-a in Bohai Sea, China," *Reg. Stud. Mar. Sci.*, vol. 66, 2023. doi: 10.1016/j.rsma.2023.103163

[72] K. Zhang, X. Zhao, J. Xue, D. Mo, and D. Zhang, "The temporal and spatial variation of chlorophyll a concentration in the China Seas and its impact on marine fisheries," *Front. Mar. Sci.*, vol. 10, 2023. doi: 10.3389/fmars.2023.1212992

Jing-wen Hu received the Ph.D degree in Marine information detection and processing from Ocean University of China, Qingdao, China, in 2016. She is currently an Associate Researcher with Shandong Marine Forecast and Hazard Mitigation Service. Her research interests include ocean remote sensing and marine disaster prevention.

Xiao-yan Liu received the M.S. degrees in Marine information detection and processing from Ocean University of China, Qingdao, China, in 2014. She has been an engineer with the Institute of Oceanographic Instrumentation, Qilu University of Technology (Shandong Academy of Sciences) since 2014. She is currently pursuing the Ph.D. degree with Ocean University of China. She is the author of about 20+ articles and holds two patents. Her research interests include ocean remote sensing and ocean optics.

Qi-xiang Wang received the Ph.D. degree in ecology from Ocean University of China, in 2009. He is currently a Researcher with Shandong Marine Forecast and Hazard Mitigation Service. His research interests include marine disaster prevention, ecological restoration, and ocean remote sensing.

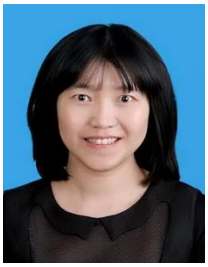

Xin Li received the M.S. degree in Engineering from Shandong University, Jinan, China, in 2011. She is currently a senior engineer at the Weifang Marine Development Research Institute. Her research interests include marine observation and forecasting, marine environmental monitoring, and marine area management.

Wen-long Dong received the Ph.D. degree in ecology from Ocean University of China, in 2016. He is currently an Associate Researcher with Shandong Marine Forecast and Hazard Mitigation Service. His research interests include marine disaster prevention, ecological restoration, and ocean remote sensing.

Wei-qi Lin, currently studying at Qilu University of Technology (Shandong Academy of Sciences). He is a Marine technology major student. He is diligent, serious and assiduous, and full of curiosity about related majors.

Jun-yue Zhang was admitted to Qilu University of Technology (Shandong Academy of Sciences) in 2023. She is currently studying in Marine technology major. She is diligent and assiduous, and interested in ocean remote sensing.

Ming-yu Li is now an undergraduate at Qilu University of Technology (Shandong Academy of Sciences), majoring in measurement and control technology and instruments (marine measurement and control direction). He is very interested in marine disaster prevention.

Zhi-hong Wu received the M.S. degree from Ocean University of China, Qingdao, China, in 2016. He is currently a Researcher with Shandong Marine Forecast and Hazard Mitigation Service. His research interests include coastal and marine ecosystem conservation and marine disaster prevention.